

Mesoporous Silica Films with Long-Range Order Prepared from Strongly Segregated Block Copolymer/Homopolymer Blend Templates

Vijay R. Tirumala,^{†,‡} Rajaram A. Pai,^{†,§} Sumit Agarwal,^{†,||} Jason J. Testa,^{†,⊥}
Gaurav Bhatnagar,[†] Alvin H. Romang,[†] Curran Chandler,[†] Brian P. Gorman,[#]
Ronald L. Jones,[‡] Eric K. Lin,[‡] and James J. Watkins^{*,†}

Polymer Science and Engineering, University of Massachusetts, Amherst, Massachusetts 01003, Polymers Division, National Institute of Standards and Technology, Gaithersburg, Maryland 20899, and Materials Science and Engineering, University of North Texas, Denton, Texas 76207

Received March 22, 2007. Revised Manuscript Received August 31, 2007

Well-ordered mesoporous silica films were prepared by infusion and selective condensation of Si alkoxides within preorganized block copolymer/homopolymer blend templates using supercritical CO₂ as the delivery medium. The morphologies of the mesoporous silica films reflect significant improvements in the strength of segregation and long-range order of template blends of poly(ethylene oxide-*b*-propylene oxide-*b*-ethylene oxide) triblock copolymers with selectively associating homopolymers such as poly(acrylic acid) or poly(4-hydroxystyrene) prior as compared to templates comprised of the neat copolymer. Control over film porosity, pore ordering, and morphology of the films is achieved through simple variations in the homopolymer concentration. The films were characterized using X-ray reflectivity, small-angle X-ray scattering, and transmission electron microscopy.

Introduction

Block copolymers are of interest as sacrificial templates for technologically important materials such as mesoporous low-dielectric-constant thin films, size-selective membranes, and other mesoporous materials.^{1–4} In one approach that relies on cooperative self-assembly, precursors such as Si alkoxides are mixed with the block copolymers in solution.^{5–10} Gelation of the precursor sols then occurs simultaneously with assembly of the copolymer surfactant and precursor species. Calcination of the resulting composite yields meso-

porous inorganic networks. Recently we reported a different approach in which inorganic network formation and template self-assembly are separated into distinct steps.¹¹ An amphiphilic block copolymer such as poly(ethylene oxide-*b*-propylene oxide-*b*-ethylene oxide) (PEO-PPO-PEO, Pluronic BASF) is first deposited onto a substrate by spin-coating from a solution containing an acid catalyst. Inorganic precursors are then infused into the preorganized copolymer thin films using supercritical CO₂ as the carrier. Swelling the template in supercritical carbon dioxide significantly enhances diffusion within the polymer film¹² without disrupting phase segregation.¹³ Precursor condensation then occurs exclusively within the acid catalyst-doped hydrophilic phase, and removal of the template yields mesoporous inorganic structures.^{14,15} Separation of template assembly from inorganic network formation offers a number of advantages, including the ability to select templates and precursors independently by elimination of the requirement of cooperative assembly. Moreover, because the template structure can be conserved in the mesoporous films, manipulation of the template prior to precursor infusion by independent patterning, domain alignment, or blending with additional components offers opportunities for further control of film morphology and composition.

* Corresponding author. E-mail: watkins@polysci.umass.edu.

[†] University of Massachusetts.

[‡] National Institute of Standards and Technology.

[§] Present address: Intel Corporation, Portland, OR.

^{||} Present address: Department of Chemical Engineering, Colorado School of Mines, Golden, CO 80401.

[⊥] Present address: General Electric Corporate Research and Development, Schenectady, NY.

[#] University of North Texas.

- (1) Urbas, A.; Sharp, R.; Fink, Y.; Thomas, E. L.; Xenidou, M.; Fetters, L. J. *Adv. Mater.* **2000**, *12*, 812–814.
- (2) Cheng, J. Y.; Ross, C. A.; Thomas, E. L.; Smith, H. L.; Vancso, G. J. *Appl. Phys. Lett.* **2002**, *81*, 3657–3659.
- (3) Segalman, R. A. *Mater. Sci. Eng. R* **2005**, *48*, 191–226.
- (4) Cheng, J. Y.; Ross, C. A.; Chan, V. Z.-H.; Thomas, E. L.; Lammertink, R. G. H.; Vancso, G. J. *Adv. Mater.* **2001**, *13*, 1174–1178.
- (5) Wu, Y.; Cheng, G.; Katsov, K.; Sides, S. W.; Wang, J.; Tang, J.; Fredrickson, G. H.; Moskovits, M.; Stucky, G. D. *Nat. Mater.* **2004**, *3*, 816–822.
- (6) Landskron, K.; Ozin, G. A. *Science* **2004**, *306*, 1529–1532.
- (7) Lu, Y.; Ganguli, R.; Drewien, C. A.; Anderson, M. T.; Brinker, C. J.; Gong, W.; Guo, Y.; Soyez, H.; Dunn, B.; Huang, M. H.; Zink, J. I. *Nature* **1997**, *389*, 364–368.
- (8) Hayward, R. C.; Chmelka, B. F.; Kramer, E. J. *Macromolecules* **2005**, *38*, 7768–7783.
- (9) Yang, P.; Zhao, D.; Margolese, D. I.; Chmelka, B. F.; Stucky, G. D. *Nature* **1998**, *396*, 152–155.
- (10) Freer, E. M.; Krupp, L. E.; Hinsberg, W. D.; Rice, P. M.; Hedrick, J. L.; Cha, J. N.; Miller, R. D.; Kim, H. C. *Nano Lett.* **2005**, *5*, 2014–2018.

- (11) Pai, R. A.; Humayun, R.; Schulberg, M. T.; Sengupta, A.; Sun, J.-N.; Watkins, J. J. *Science* **2004**, *303*, 507–510.
- (12) Gupta, R. R.; RamachandraRao, V. S.; Watkins, J. J. *Macromolecules* **2003**, *36*, 1295–1303.
- (13) Vogt, B. D.; Brown, G. D.; RamachandraRao, V. S.; Watkins, J. J. *Macromolecules* **1999**, *32*, 7907–7912.
- (14) Pai, R. A.; Watkins, J. J. *Adv. Mater.* **2006**, *18*, 241–245.
- (15) Vogt, B. D.; Pai, R. A.; Lee, H. J.; Hedden, R. C.; Soles, C. L.; Wu, W. L.; Lin, E. K.; Bauer, B. J.; Watkins, J. J. *Chem. Mater.* **2005**, *17*, 1398–1408.

We have recently reported surprising enhancements in phase segregation and long-range order in PEO-PPO-PEO Pluronic copolymers blended with homopolymers that exhibit strong interactions with the PEO block through hydrogen bonding including poly(acrylic acid) (PAA) and poly(4-hydroxystyrene) (PHS).¹⁶ Increased order upon blending is due in part to the inhibition of crystallization at room temperature but is primarily due to an increase in the segregation strength between block copolymer domains in the melt. The advantages of stronger segregation strength in the blend template are twofold: higher degrees of order compared to the weakly segregated copolymer and the potential to produce smaller domains by inducing phase segregation in low molecular weight copolymers. These advantages should carry over to the templated silicas. In this work, we show that this is indeed the case and that infusion and phase selective condensation of silica precursors within one domain of strongly segregated templates comprised of blends of commercial PEO-PPO-PEO triblock copolymer surfactants with strongly associating homopolymers yield mesoporous silicas with excellent long-range order. The template morphology and strength of segregation can be controlled as a simple function of homopolymer concentration and the nature of its interactions. When combined with the infusion of silica precursors from supercritical carbon dioxide, this approach provides control over the properties of mesoporous silica films through their long-range order, total porosity, and morphology.

Experimental Section¹⁷

Materials. Pluronic F127 triblock copolymer (PEO₁₀₆-PPO₇₀-PEO₁₀₆) and PAA (molecular weight = 2000 g mol⁻¹) were purchased from Aldrich Chemical Co. PHS (molecular weight = 8000 g mol⁻¹) was purchased from Polysciences, Inc. Tetraethylorthosilicate (TEOS) and *p*-toulene sulfonic acid (*p*TSA) were obtained from Acros Chemicals. Carbon dioxide (Coleman grade) used in the infusion process was obtained from Merriam-Graves. Ethanol and propylene glycol monoether acetate (PGMEA) were obtained from Pharmco Inc. All chemicals were used as received without further purification. In-house deionized water was used for the infusions.

Thin films of blend templates were prepared by solution casting or spin-coating onto silicon wafer a mixture of block copolymer and homopolymer dissolved in a common solvent at a given mass fraction. Ethanol and a 50:50 mixture of ethanol/PGMEA were used as common solvents for PAA and PHS blends, respectively.

Infusion of Silica Alkoxide Precursors. Highly ordered mesostructured silica films were prepared by the phase selective condensation of Si alkoxides within preorganized blend templates in supercritical carbon dioxide as reported earlier.¹¹ The blend films containing *p*TSA catalyst were prepared by spin coating onto Si wafers and then exposed to a solution of the precursors in humidified supercritical carbon dioxide at 60 °C and 123 bar for 2 h. The reactor was then slowly depressurized to atmospheric

pressure to yield a uniform, defect-free, mesostructured film. The organic template was subsequently removed by calcination at 400 °C for 6 h in air with a heating/cooling rate of 1 °C/min for the temperature ramps.

Characterization. Fourier transform infrared spectroscopy (FTIR) absorption spectra of spin-cast blend films were collected on a BioRad ExCalibur spectrometer in the wavenumber range 400–4000 cm⁻¹ with a spectral resolution of 4 cm⁻¹. The data reported for each sample were obtained by a coaddition of 200 independent scans to increase the signal-to-noise ratio. The sample spectra were obtained by using films of high resistivity (undoped) silicon wafers after subtracting the spectrum of a blank wafer. Differential scanning calorimetry (DSC) thermograms were measured using a Q1000 DSC (TA Instruments) by first heating the sample from -40 to 100 °C followed by subsequent cooling and heating cycles at the rate of 5 °C/min. The samples were solution cast on glass slides, air-dried for a day, and finally left under vacuum overnight prior to analysis. Atomic force microscopy (AFM) height and phase images were acquired using a Digital Instruments Dimension 3000 scanning microscope in the tapping mode. Blend films were spin-cast on silicon wafers from solution to be approximately 500 nm thick. Specular X-ray reflectivity (XRR) from as-infused composite films and mesoporous silica films was measured using a Phillips PW3040-MPD diffractometer using Cu K α radiation in a θ -2 θ configuration. Mass density profiles were obtained by modeling the XRR profiles below the critical angle of silicon at $q_z < 0.0032 \text{ \AA}^{-1}$. Small-angle X-ray scattering (SAXS) measurements to characterize the morphology of mesoporous silica films synthesized on a 300- μm -thick silicon wafer were taken at the beamline 5-ID, Advanced Photon Source, using X-rays of 13 keV incident energy ($\lambda \approx 0.9 \text{ \AA}$) in transmission mode with a sample-to-detector distance of 2.92 m. Transmission electron microscopy (TEM) was performed on a JEOL 2000FX electron microscope operating at 200 kV. The mesostructured silica films were scraped off the substrate using a razor blade, ground to form dilute slurry with ethanol or acetone, and then dropped onto Formvar coated copper grids (Electron Microscopy Sciences). The grids were then dried in air for at least 1 h prior to observation in the transmission electron microscope.

Results and Discussion

We first investigated the influence of adding low molar mass PAA or PHS homopolymers to weakly segregated semicrystalline Pluronic F127 (henceforth referred to as F127) block copolymer (PEO₁₀₆-PPO₇₀-PEO₁₀₆) template films. Previous studies on PAA/PEO homopolymer blends have shown that hydrogen-bonding interactions between the carboxylic acid groups and the ether oxygen in PEO suppress PEO crystallization.^{18,19} Recent small-angle neutron scattering results have shown that PAA is selectively miscible with the PEO segments in Pluronic copolymers.²⁰

We studied the molecular-level interactions between PAA and F127 using FTIR and DSC. The effect of PAA on the long-range template order at room temperature was then examined using AFM. Figure 1a shows FTIR spectra of a series of PAA/F127 blends. With increasing PAA concentration, we observed an increase in intensity of an absorption

(16) Tirumala, V. R.; Romang, A. H.; Agarwal, S.; Lin, E. K.; Watkins, J. J. *Adv. Mater.*, under review.

(17) Certain equipment, instruments or materials are identified in this paper to adequately specify the experimental details. Such identification does not imply recommendation by the National Institute of Standards and Technology nor does it imply the materials are necessarily the best available for the purpose.

(18) Lu, X.; Weiss, R. A. *Macromolecules* **1995**, *28*, 3022–3029.

(19) Moskala, E. J.; Howe, S. E.; Painter, P. C.; Coleman, M. M. *Macromolecules* **1984**, *17*, 1671–1678.

(20) Tirumala, V. R.; Vogt, B. D.; Lin, E. K.; Watkins, J. J. *Abstr. Pap. Am. Chem. Soc.* **2006**, 231:POLY.

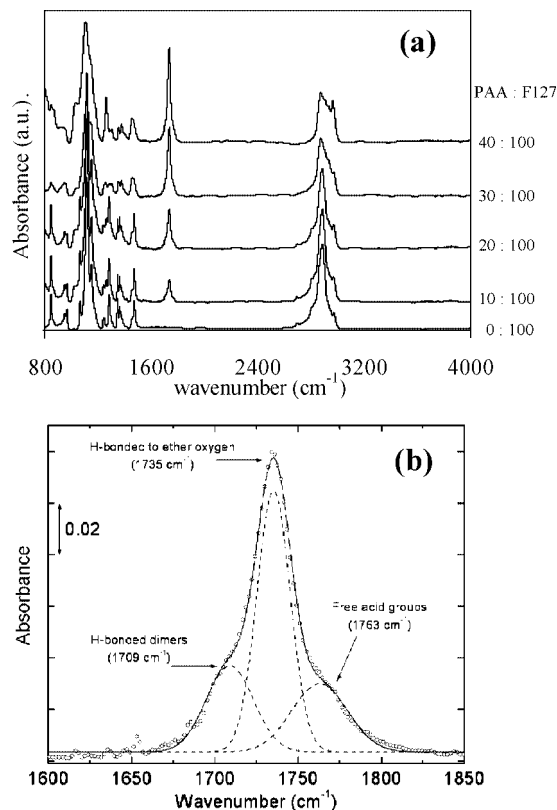


Figure 1. (a) FTIR spectra for spin-coated films of F127 and its PAA blends at various compositions. (b) Deconvoluted spectrum of C=O stretching vibrations from a 40:100 PAA:F127 blend showing the relative contributions from different interactions of COOH groups in PAA and the ether oxygen in F127.

band centered at 1735 cm^{-1} . This band is associated with the C=O stretching vibrations in carboxylic acid groups of PAA that are hydrogen bonded to the ether oxygen of PEO or PPO. For the absorption spectrum of a 40:100 mass ratio of a PAA/F127 blend, the absorption peak at 1735 cm^{-1} has two shoulders centered at 1709 cm^{-1} and 1763 cm^{-1} (Figure 1b). In the polymer blend, PAA can (a) interact with the ether oxygen of PEO or PPO via hydrogen bonding ($\text{H}_3\text{C}\{\text{CH}_2\text{CH}_2\text{---O}\cdots\text{HOOC}\}_n\text{CH}_3$), (b) exist in a self-hydrogen-bonded cyclic dimer state ($\text{HOC---O}\cdots\text{HOOC}$), or (c) remain as unbound free acid (C=O). The absorption spectrum shown in Figure 1b was deconvoluted²¹ using Gaussian line shapes to incorporate the respective contributions of these three C=O bonding configurations. From the deconvolution of the absorption spectrum, we find that approximately 78% by volume of the PAA was hydrogen bonded to ether oxygen atoms indicating molecular-level mixing in the homopolymer–block copolymer blend. The addition of PAA to the F127 template also decreases the melting point of crystalline PEO and affects its crystal growth behavior. Figure 2a shows DSC thermograms of neat F127 and PAA/F127 blends at different blend compositions. The melting point of PEO (endotherm peak position) and its melting enthalpy (integrated area under the peak) in the blend templates decreases with increase in PAA concentration

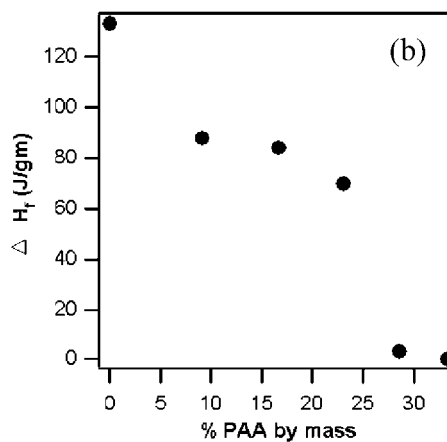
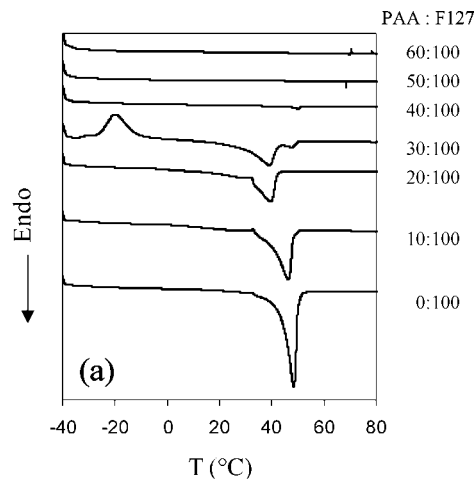


Figure 2. (a) DSC thermograms and the calculated (b) heat of fusion of F127 and its PAA blends at various compositions normalized with respect to PEO mass fraction.

(Figure 2b), indicating miscibility of PAA and the PEO block. PEO crystallization was completely suppressed above a critical blend composition of 30% PAA by mass (PAA/F127 = 43:100).

Figure 3 shows AFM images of blend templates at different PAA concentrations acquired at room temperature. The microphase-separated neat F127 template has a randomly oriented cylindrical morphology. The number of cylinders aligned along the same direction increases with the addition of PAA. The average grain size in each template was visually identified as the area encompassing the microphase separated cylinders oriented in the same direction. It was found to increase gradually from approximately $0.04\text{ }\mu\text{m}^2$ in a neat F127 template (Figure 3a) to approximately $1\text{ }\mu\text{m}^2$ in the blend template with 28.5% PAA by mass (Figure 3c). The increased grain size in blend templates is in part a consequence of suppressing PEO crystallization at room temperature through blending with PAA. However, using SAXS and small-angle neutron scattering, we found that PEO-PPO-PEO blends with homopolymers that can hydrogen bond with the PEO domain exhibit strong segregation in the melt relative to the neat copolymer, suggesting that improved order is not solely a consequence of suppressing PEO crystallization kinetics but is thermodynamically favored.¹⁶ Similar results are expected from blends of Pluronic copolymers with PHS because the latter is also known to strongly interact with the homopolymer PEO via hydrogen bonding.²²

(21) Lee, J. Y.; Painter, P. C.; Coleman, M. M. *Macromolecules* **1988**, *21*, 346–354.

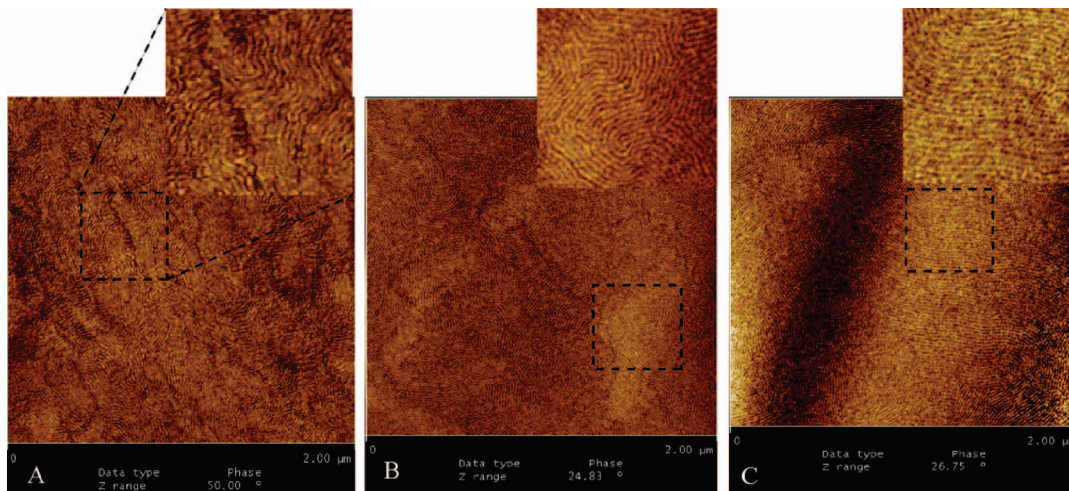


Figure 3. AFM phase images ($2 \mu\text{m} \times 2 \mu\text{m}$) for spin-coated films of (A) neat F127 and its PAA blends at (B) 16.67% and (C) 28.5% by mass. Insets show magnified regions of $0.5 \times 0.5 \mu\text{m}^2$ from highlighted areas for clarity.

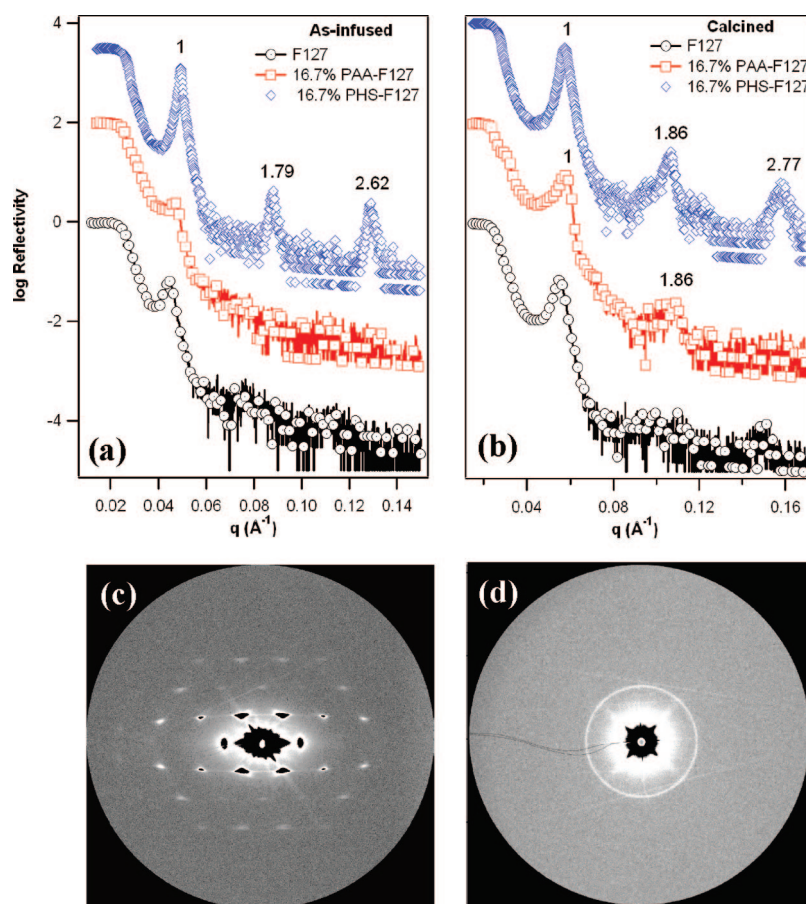


Figure 4. XRR profiles of (a) the as-infused composite films and (b) mesoporous silica films templated from neat F127 and its blends with PAA and PHS at 16.7% by mass. Parts c and d show the 2D SAXS detector images measured at 10° and 90° angles of incidence relative to the surface, respectively, of the mesoporous film templated from PHS/F127 blend shown in part b.

The well-ordered block copolymer/homopolymer blends are useful templates for mesoporous silica. “As-infused” silica/polymer composites are prepared by selectively condensing silica within the acid doped, hydrophilic PEO-rich matrix via TEOS infusion from supercritical carbon dioxide at 60°C and 123 bar. At these conditions, the template blend is in the melt phase and is diluted slightly with CO_2 . But the microphase morphology is preserved in the melt phase as elaborated in ref 16. Mesoporous silicas were prepared by

calcination of the composite template films at 400°C for 4 h in air. The morphology and mass density of mesoporous silica films prepared from templates of PAA/F127 and PHS/F127 blends were measured using XRR and SAXS.

Figure 4 shows the XRR profiles of the as-infused (Figure 4a) and the corresponding mesoporous silica (Figure 4b) films prepared from a neat F127 template and its blends with

PAA and PHS at 16.7% by mass. The reflectivity profiles of all samples are dominated by Bragg diffraction peaks due to the strongly correlated periodic density fluctuations of PPO cylinders oriented parallel to the substrate. The absence of the high frequency Kiessig fringes associated with a finite film thickness is likely due to the interfacial roughness on the order of 200 Å at the film–air interface. The templated order in the as-infused films and the mesoporous silicas can be determined from the presence of zero-, first-, and second-order reflections. The ratio of primary reflection wavevector to that of the higher order reflections from the as-infused composites and the mesoporous silica films (1:1.79:2.62; 1:1.86:2.77) is consistent with a cylindrical morphology oriented parallel to the substrate. As a result of the anisotropic changes in film thickness during infusion and calcination, the cylinders oriented parallel to the substrate are compressed slightly from the ideal hexagonally close packed geometry. This change was confirmed by measuring the transmission X-ray scattering at multiple angles of incidence. Figure 4c shows the two-dimensional (2D) SAXS profile of the film templated from PHS/F127 blend measured at a 10° angle of incidence with respect to the surface. We observe hexagonally distributed diffraction spots with a slight anisotropy that suggests that the majority of the cylindrical mesopores are oriented parallel to the substrate. At angles of incidence greater than 80°, a single isotropic scattering ring was observed suggesting that cylindrical mesopores are randomly oriented in the plane of the film (Figure 4d). In comparison, for a film with more randomly oriented cylindrical mesopores, diffraction spots were not observed above the 45° angle of incidence.²³ The scattering results were confirmed further by TEM on the cross section of the silica film. The cylindrical mesopores are predominantly oriented parallel to the substrate through the entire film thickness as shown in Figure 5a. In comparison, cylindrical mesopores in the silica film prepared from neat F127 template are randomly oriented with only a few ordered layers at the film–substrate and film–air interfaces (Figure 5b).

The primary peak position (q^*) in XRR corresponds to the domain spacing of cylindrical mesopores oriented parallel to the substrate, and the critical angle (q_c^2) of the film is proportional to the average mass density of the film. The domain spacing (d) of the as-infused and mesoporous silica films prepared from different blend templates measured using XRR are given in Table 1. The primary peak position of as-infused composite films changes from 0.044 Å⁻¹ ($d_{F127} \approx 142.3$ Å) in neat F127 to 0.047 Å⁻¹ ($d_{PAA/F127} \approx 132.9$ Å) and 0.049 Å⁻¹ ($d_{PHS/F127} \approx 127.5$ Å) in those of PAA and PHS blends, respectively. The corresponding d -spacings measured from the mesoporous silica films are 0.055 Å⁻¹ ($d_{F127} \approx 113.7$ Å), 0.058 Å⁻¹ ($d_{PAA/F127} \approx 108.1$ Å), and 0.0574 Å⁻¹ ($d_{PHS/F127} \approx 109.5$ Å), respectively. The slight decrease in d of mesoporous silicas prepared from the blends relative to neat F127 is accompanied by an increase in the long-range template order. These results suggest that the domain segregation between PEO and PPO is improved with the addition of strongly interacting homopolymer.

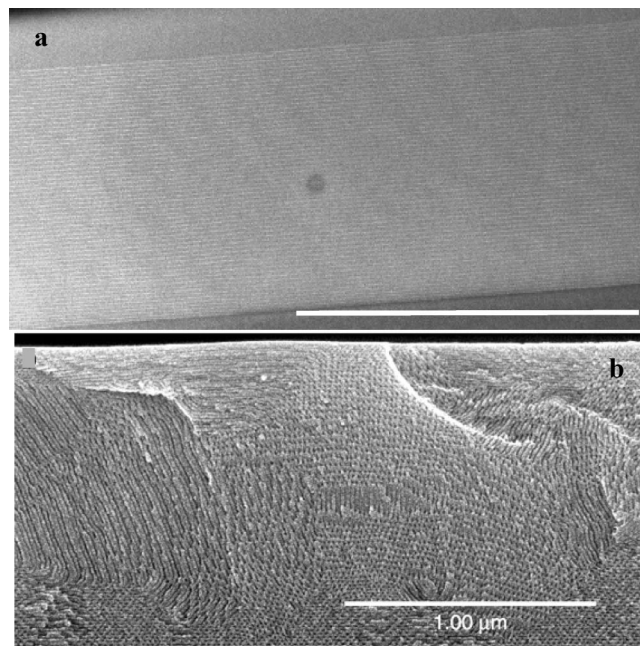


Figure 5. (a) Cross-sectional transmission electron micrograph of the mesoporous silica film prepared from PHS/F127 blend template at 16.7% PHS by mass. For comparison, (b) the cross-sectional scanning electron micrograph of the mesoporous silica film prepared from the neat F127 template is reprinted with permission from ref 12. Copyright 2004 AAAS. Bar = 1 μm.

After condensation of the silica precursor in the swollen template, calcination at 400 °C causes the final mesoporous silica film to shrink in thickness when compared to the as-infused composite film. The shrinkage in films prepared at different PAA and PHS blend compositions calculated from the difference in d -spacing between composite and mesoporous silica films is given in Table 1.²⁴ In addition to improved domain segregation, blending F127 with either PAA or PHS reduced film shrinkage during calcination. The lower film shrinkage in mesoporous silica films templated from blends should result in greater porosity compared to those templated from neat F127 if blending does not affect the precursor infusion and condensation process. This premise can be assessed from the critical angle for reflected intensity as measured using XRR, which is proportional to the average mass density of the film.

The reflected intensity from the as-infused and mesoporous films decayed gradually with wavevector in the critical angle region. A gradual decrease in reflected intensity corresponds to a film with a slight mass density gradient through its thickness. The experimental XRR profiles can be modeled using a one-dimensional Schrödinger equation in the Paratt formalism^{25,26} to estimate the density gradients through the film thickness. On the basis of the model parameters, the mass density of all the films increased through their thickness and had the same maximum density at the film–substrate

(23) Vogt, B. D.; Lee, H.-J.; Wu, W. L.; Liu, Y. *J. Phys. Chem. B* **2005**, *109*, 18445–18450.

(24) Film shrinkage upon calcination of mesoporous silicas prepared by the SCF infusion method can be substantially reduced by increasing the precursor infusion temperature. For example, less than 6% shrinkage was observed by increasing the infusion temperature to 90°C. Pá, R. A. Ph.D. Thesis, University of Massachusetts, 2005.

(25) Ankner, J. F.; Maikrzak, C. F. *Proc. SPIE* **1992**, *1738*, 260–269.

(26) Paratt, L. G. *Phys. Rev.* **1954**, *95*, 359–369.

Table 1. Domain Spacing d ($=2\pi/q^*$; Å) in Polymer/Silica Composite and Mesoporous Silica Films Prepared from the F127 Blend Templates, As Calculated from the Primary Peak Position (q^*) in XRR^a

homopolymer % by mass	d -spacing (Å)					
	as-infused composite		mesoporous silica		shrinkage ^b	
	PAA/F127	PHS/F127	PAA/F127	PHS/F127	PAA/F127	PHS/F127
0	142.75	140.91	114.76	114.76	27.99	27.99
16.7	132.86	127.49	108.14	109.48	24.72	18.3
28.5	124.97	127.49	104.79	114.6	20.18	13.62
37.5	132.46	130.50	113.71	114.89	18.75	15.61

^a The uncertainty associated with fitting the peak position is less than 0.1% but does not include the errors from changes in instrumental background.

^b See ref 24.

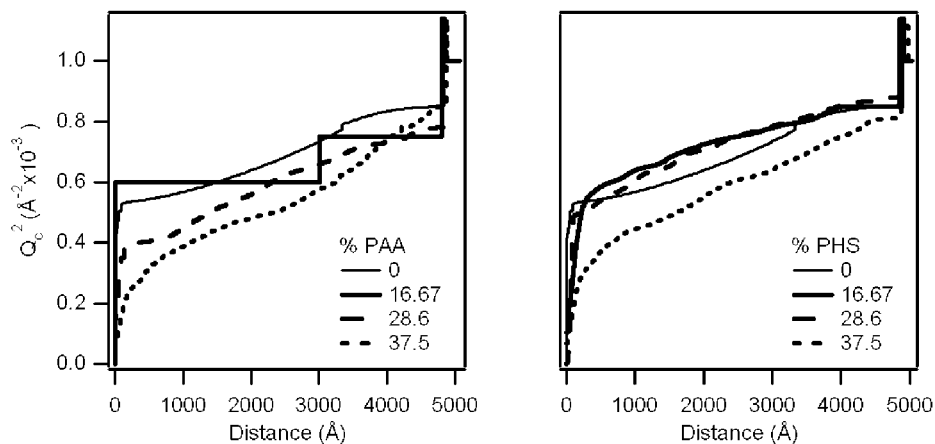


Figure 6. q_c^2 profiles of the mesoporous silica films templated from F127 blended with PAA and PHS, calculated by modeling the XRR curves.

interface irrespective of template composition. The density gradients changed with concentration for each homopolymer as observed from the q_c^2 profiles shown in Figure 6. The average mass density of mesoporous films templated from PAA/F127 blends decreased (porosity increased) by increasing PAA concentration. The increased porosity in mesoporous silicas templated from PAA/F127 blends will lower the average dielectric constant of the film, a parameter critical for semiconductor applications. The mass density of mesoporous silicas templated from PHS/F127 blends, on the other hand, did not change appreciably with blend composition except at the highest concentration studied.

Similar results were obtained for as-infused composites and mesoporous silicas prepared from Brij [poly(EO_m-ethylene_n)] copolymer templates blended with PAA and PHS. The added homopolymers selectively interact with PEO via hydrogen bonding but are immiscible with polyethylene. However, the addition of homopolymer also induced a change in microphase morphology of the silica films templated by the Brij copolymer blends. Mesoporous silicas prepared from neat Brij 78 copolymer template exhibit a cubic mesostructure as shown previously.^{14,27} TEM images and the corresponding electron diffraction patterns of mesoporous silica films templated from the PAA blend at 28.5% by mass show a hexagonally packed cylindrical morphology (Figure 7). Similar to that observed in F127 blends, the mesoporous silica film templated from Brij 78 copolymer blended with PHS is better ordered than that obtained from

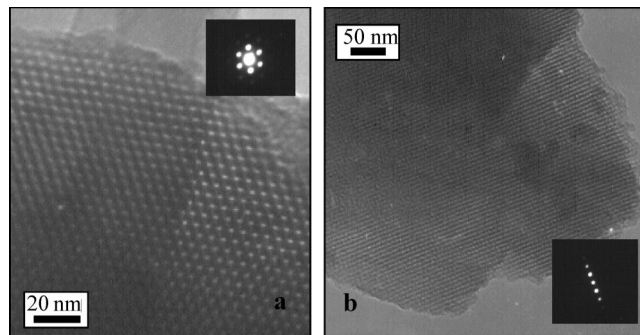


Figure 7. TEM lattice images of mesoporous silicas templated by Brij 78 copolymer blended with PAA at 28.5% by mass. Insets in parts a and b are the corresponding electron diffraction patterns and clearly show the hexagonally close packed cylindrical morphology. SAXS data from the mesoporous film at 70° incident angle that confirms the morphology is provided in the Supporting Information.

blending with PAA. Specular XRR measurements (not shown here) demonstrate that the mesoporous silicas templated from Brij copolymer blended with PAA and PHS exhibit a remarkable similarity in mass density gradients through the film thickness with those in silicas templated from F127 blends. Films templated from PHS/Brij 78 blends also exhibit reduced shrinkage relative to those from PAA/Brij 78 at the same composition, as evidenced from the relatively smaller change in d -spacing between the as-infused composite and its corresponding mesoporous silica (Table 2). The improved long-range order and reduced shrinkage in mesoporous silica films prepared from the blend templates may translate into better mechanical properties, a criterion necessary for the films to survive the various procedures involved in semiconductor device fabrication.

(27) Kim, J. M.; Sakamoto, Y.; Hwang, Y. K.; Kwon, Y.-U.; Terasaki, O.; Park, S. E.; Stucky, G. D. *J. Phys. Chem. B* **2002**, *106*, 2552–2556.

Table 2. Domain Spacing d ($=2\pi/q^*$; Å) in Polymer/Silica Composite and Mesoporous Silica Films Prepared from the Brij78 Blend Templates, As Calculated from the Primary Peak Position (q^*) in XRR^a

sample	d -spacing (Å)		
	as-infused composite	mesoporous silica	shrinkage ^b
Brij 78	73.5	62.44	11.06
16.7% PAA/Brij 78	68.57	56.89	11.68
16.7% PHS/Brij 78	65.9	63.48	2.42

^a The uncertainty associated with fitting the peak position is less than 0.1% but does not include the errors from changes in instrumental background. ^b See ref 24.

Conclusion

We have shown that the long-range order in mesoporous silicas produced by phase selective condensation of silica precursors within preorganized block copolymer films can be enhanced dramatically when the amphiphilic block copolymer templates are blended with strongly interacting homopolymers prior to precursor infusion. The improvements in the mesoporous film structure reflect stronger phase segregation in the copolymer/homopolymer blends as compared to the neat copolymer templates. This approach

provides a simple strategy for tuning template morphology, order, and the degree of domain segregation through controlled addition of a homopolymer. The nature and concentration of the homopolymer can serve as additional parameters to control the total porosity of mesoporous silicas templated from block copolymer/homopolymer blends.

Acknowledgment. This work was supported by funding from the National Science Foundation under Grant CTS-0304159 and by the NSF Center for Hierarchical Manufacturing (DMI-0531171). Facilities supported by the NSF Materials Research Science and Engineering Center at UMass are gratefully acknowledged. Use of beamline 5-ID at the Advanced Photon Source was partly supported by the Department of Energy, Office of Science, Basic Energy Sciences, under Contract No. W-108-ENG-31.

Supporting Information Available: Transmission electron micrographs of mesoporous silica films prepared from poly(oxyethylene-*b*-ethylene) copolymers blended with PAA along with corresponding electron diffraction and 2D SAXS patterns at 70° incident angle (PDF). This material is available free of charge via the Internet at <http://pubs.acs.org>.

CM070792X